ISSN 1846-6168 (Print), ISSN 1848-5588 (Online)
https://doi.org/10.31803/tg-20241221135943

Original scientific paper
Received: 2024-12-21, Accepted: 2025-02-17

Impact of Infill Pattern Design on Stress-Strain behaviour of 3D Printed Parts

Rrahim Sejdiu, Xhemajl Mehmeti*, Flamur Salihu, Labinot Topilla, Drin Krasniqi, Mohamad El Mehtedi, Agron Bajraktari

Abstract: Compared to some conventional manufacturing processes, the properties of additive manufacturing parts can depend on the structural and manufacturing process parameters, rather than just on the type of materials used. The purpose of this paper is to evaluate the tensile mechanical properties of the components printed with a 3D printer by changing the design of the infill pattern. The study presents the data of 13 (by 3 tests for each form of filling) different infill pattern designs, prepared and tested according to the ISO 527-2:2012 standard. The samples were analyzed according to the paired sample tests, considering the weight and the results of the tests, as well as the impact of the infill pattern on the test results. Significant differences were observed among the samples in terms of engineering stress and strain. The line infill pattern demonstrated better results in the engineering strain whereas the concentric infill pattern yielded superior values for engineering stress. Regarding ultimate tensile strength, concentric infill pattern shows significantly higher results than all other samples. Taking into consideration the results of the samples, it is concluded that there are significant differences between the design of the infill pattern and the other analyzed studies, which should be considered depending on the intended use of the 3D printed elements.

Keywords: infill pattern; tensile strain; tensile stress; tensile strength; 3D printing

1 INTRODUCTION

The 3D printing industry has taken a huge leap of development in recent years. This technique involves producing solid objects from digital files, which has garnered the attention of various industries, along with the scientific and academic communities. The development trend of this technology is versatile, and it is difficult to accurately predict the future of its development. This is because 3D printers are successfully utilized across various fields such as medicine, engineering, architecture, construction, and design [1-3]. The easy and fast possibilities of printing complex shapes [4], have made this technology develop rapidly in all branches of industry [5]. The global 3D printing market is estimated to be worth USD 20.37 billion in 2023, and according to CAGR (Compound Annual Growth Rate) prediction, the 3D printing industry will grow by 23.5% from 2024 to 2030 (Horizon, 2024).

The advantages of 3D technologies allow not only researchers and experts, but also passionate individuals who use 3D printers to easily produce prototypes of their ideas, since 3D printing greatly simplifies prototype production. This technology has reduced product design and manufacturing processes from weeks to days or even hours.

With the increase in popularity of 3D printing technologies, different materials have been developed which comprise a wide range, including: PLA (Polylactic Acid), ABS (Acrylonitrile Butadiene Styrene), PETG (Polyethylene Terephthalate Glycol), TPU (Thermoplastic Polyurethane), Nylon, Carbon Fibre Filled Filaments, and Wood-Filled Filaments [6].

The most commonly used materials in 3D printing are polymers, due to their versatility, low cost, ease of use and in some cases, environmental friendliness [7, 8]. These materials can be melted and extruded into different shapes [9]. Polylactic Acid Composites (PLA) are one of the most widely used raw materials for 3D printing, mainly because of their environmentally friendly characteristics, low cost, high-quality printed surface, and properties that are relatively similar to those of other commonly used printing materials [7].

Due to variety of use and growing trends of 3D printing products [10], it is important to understand their mechanical properties. During practical applications, products must withstand different levels of mechanical loads, therefore, it is important to know the durability of parts for each application [11].

According to the ASTM F2792 standard, 3D printing technologies are divided into seven groups, including: the binding jetting, directed energy deposition, material extrusion, material jetting, powder bed fusion, sheet lamination and vat photopolymerization [12, 14].

The mechanical properties of materials that are determined experimentally are very important during the product design phase.

The most frequent causes of structural failures generally are divided into two categories:

1) Negligence during the design, construction or operation of the structure and,
2) Applying new design or new materials, which may show unexpected results [15].

The test results are used to determine the dimensions of elements produced, as well as the domain of their use. In general, one of the most important mechanical properties of materials is their stability when subjected to tensile stress. The test results are used to determine the appropriate material that fulfills specific needs and to predict the behaviour of products to mechanical loads. The mechanical properties measured are yield strength, tensile strength, elongation and modulus of elasticity [16].

Various studies show that the mechanical properties of products printed with 3D technologies vary depending on the printing parameters, which include: Shell (wall thickness), speed of print, material (printing temperature, type of materials), and infill (density, patterns, infill line distance [5, 7, 14, 17-20] etc. Furthermore, extruder temperatures, print platform (bed) temperature, extruder head diameter, and print

head closure [21] are also important factors influencing the mechanical properties of printed parts.

By carefully selecting the right combination of parameters in the printing process, it becomes possible to produce products with the best characteristics.

Taking into account the many factors that affect the mechanical properties of printed products, this paper's primary objective is to investigate the impact of infill patterns on the mechanical properties of products printed with 1.75mm PLA filament using 3D printers. Furthermore, the aim of the study was to investigate the samples built from similar material for different structural design. Tensile tests were used in order to identify the strain, deformations and Young's Modulus of the samples for different loads.

During 3D printing, various factors, (such as material type, printing speed, print head diameter, printing temperature, and layer deposition) affect the mechanical properties of the printed parts, which can also vary based on the infill pattern. The infill pattern plays an important role in durability, weight and print time. It can vary depending on many parameters, including design, density and print speed. Furthermore, depending on the types of printers and the software available on the market, a considerable number of infill patterns exist.

2 MATERIALS AND METHODS (EXPERIMENTAL PART)

Poly Lactic Acid (PLA) material was used for printing the samples. According to ISO 1183 and GB/T 1033 standards, the density of this type of material, measured at 21 °C, is 1.17 g/cm³. The material used in the study is "pine green" produced by 3DHUB Company, with a diameter of 1.75 mm. G-codes samples were generated using Creality Slicer 4.8.2. and were printed on the Eder-3 V2 Neo printer (Fig. 3a). Based on the equation b Tab. 1, the length of l_2 is calculated to be 109.33 mm; 109 mm is acquired. Infill pattern designes used in this study was carried out according to the standard ISO 527-2:2012, Figs. 2a, 2b and 2c. The paper presents the test results for 39 samples (3 samples for each type of infill pattern) that were produced using the same printing parameters, except for the infill pattern (Fig. 1a - 1m), which analyzes 13 different forms of infill patterns offered by the printer software. Apart from the infill pattern parameter, other parameters for all samples were constant: standard quality 0.2 mm; wall line count 2; top and top/bottom (outline thickness) thickness 0.8 mm; top/bottom (outline thickness) layers 4; top/bottom pattern – line; infill density 30 %; printing temperature 215 °C; built plate temperature 60 °C; print speed of 50 mm/s; infill speed 60 mm/s; and travel speed of 120 mm/s.

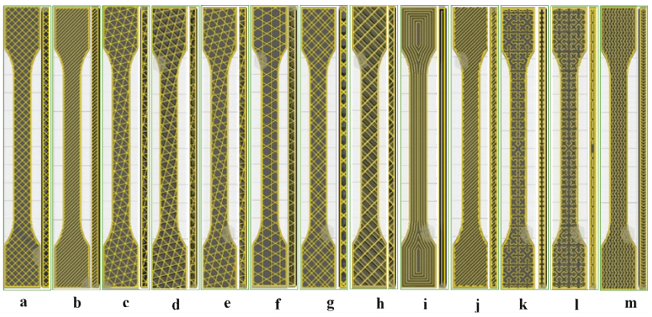

Figure 1 Infill pattern design (top and side view): a) Grid, b) Line, c) Triangle, d) Trihexagon, e) Cubic, f) Cubic Subdivision, g) Octet, h) Quarter Cubic, i) Concentric, j) Zig Zag, k) Cross, l) Cross 3D, m) Gyroid.

The tests were conducted using the WDW-50Y Stiffness Testing Machine in the laboratory of "FERPLAST", a company that produces plastic pipes and is certified according to the SK EN ISO/IEC 17025:2018 standard. Sample testing was done according to the ISO 527-2-2012 standard. Prior to the start of the tests, the samples were placed in the test environment which were prepared according to the ISO 9969 standard.

Table 1 Specimen dimensions according to ISO 527-2:2012

	Specimen type	1A (mm)	1B (mm)
l_3	Overall length	170.0	≥150.0
l_1	Length of narrow parallel-sided portion	80.0 ± 2.0	60,0 ± 0.5
r	Radius	24.0 ± 1.0	60,0 ± 0.5
l_2	Distance between broad parallel-sided portions b	109.3 ± 3.2	108.0 ± 1.6
b_2	Width at ends	20.0 ± 0.2	
b_1	Width at narrow portion	10.0 ± 0.2	
h	Preferred thickness	4.0 ± 0.2	
L_0	Gauge length (preferred) Gauge length (acceptable if required for quality control or when specified)	75.0 ± 0.5 50.0 ± 0.5	50.0 ± 0.5
L	Initial distance between grips	115 ± 1	115 ± 1
a) The recommended overall length of 170 mm of the type 1A is consistent with ISO 294-1 and ISO 10724-1. For some materials, the length of the tabs may need to be extended (e.g. l_3 = 200 mm) to prevent breakage or slippage in the jaws of the testing machine. b) $l_2 = l_1 + [4r(b_2 - b_1) - (b_2 - b_1)2]1/2$, resulting from l_1, r, b_1 and b_2, but within the indicated tolerances.			

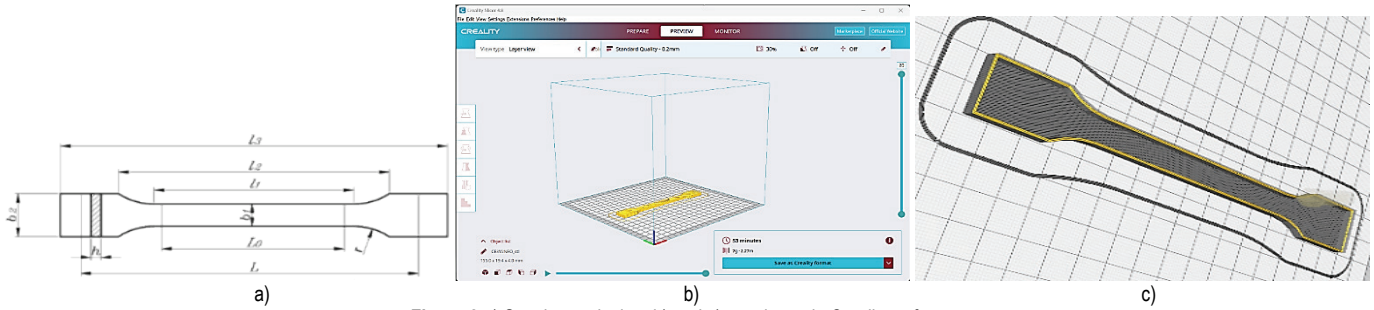

a) b) c)

Figure 2 a) Speciment design, b) and c) speciment in Creality software

Table 2 Average weight of printed samples (g) according to infill pattern.

Weight of samples													
	Grid	Lines	Triangle	Tri_hexagon	Cubic	Cubic_subdivision	Octet	Quarter_cubic	Concentric	Zig_zag	Cross	Cross_3d	Gyroid
Mean g	5.878	5.882	5.895	5.883	5.792	5.654	5.487	5.884	5.765	5.870	5.821	5.722	5.932
Std. Dev	.1328	.1233	.0575	.1028	.1078	.0855	.3430	.1036	.0923	.2097	.0751	.0862	.0880

Figure 3 a) Printing samples; b) Weighing the samples; c) Printed samples; d) Specimens during tensile testing; e) Tested samples (broken)

Table 3 Average of samples tested according to infill pattern

	Grid	Line	Triangle	Tri_hexagon	Cubic	Cubic_s_Div.	Octet	Quarter_cubic	Concentric	Zig-Zag	Cross	Cros 3D	Gyroid
Sample ID	1	2	3	4	5	6	7	8	9	10	11	12	13
Width (mm)	9.9	10	10	10	10	10	9.9	10	10	10	10	10	10
S_o (mm^2)	37.6	38.0	38.0	39.0	39.0	39.0	37.6	39.0	39.0	39.0	39.0	39.0	39.0
Strain→Force (kN)	0.2	0.2	0.2	0.2	0.2	0.2	0.2	0.2	0.3	0.2	0.2	0.2	0.2
Yield Stress σy (MPa)	20.1	19.2	22.0	20.8	22.0	21.5	19.4	20.2	25.4	19.0	18.8	19.7	20.3
Break Force F_b (kN)	0.7	0.7	0.7	0.6	0.8	0.8	0.7	0.8	0.9	0.7	0.6	0.7	0.8
Elongation at Break e_b (mm)	2.4	3.4	3.2	3.1	3.5	4.0	2.8	3.4	4.1	3.2	2.8	3.5	4.7
E_t (MPa)	646.0	617.8	621.3	639.3	628.0	585.3	650.3	639.8	734.8	641.5	623.8	642.2	640.7
Thickness (mm)	3.8	3.8	3.8	3.9	3.9	3.9	3.8	3.9	3.9	3.9	3.9	3.9	3.9
L_o (mm)	50	50	50	50	50	50	50	50	50	50	50	50	50
Set Strain x (%)	1	1	1	1	1	1	1	1	1	1	1	1	1
Grid	0.8	0.7	0.8	0.8	0.9	0.8	0.7	0.8	1.0	0.7	0.7	0.8	0.8
Yield Strain e_y (%)	4.8	4.7	6.7	5.7	6.4	6.4	4.2	6.8	6.4	4.8	4.5	5.5	4.7
Break Stress sb (MPa)	19.7	18.9	17.3	14.3	19.5	21.0	18.3	19.8	23.6	18.7	15.6	19.1	19.2
e_b (%)	4.8	6.9	6.4	6.2	7.1	8.1	5.5	6.9	8.3	6.5	5.5	7.0	9.3
Mass (g)	5.7	4.4	3.6	5.1	28.0	4.3	5.6	4.8	5.5	5.4	5.4	5.6	5.1

Table 4 Paired sample test according to Weight and Ultimate_Tensile_Strength_MPa; Engineering_Strain_mm; Strain_Force_kN; Break_Stress_Sb_MPa; Elongation_eb_percent; Tensile_Modulus_Et_MPa

Paired Samples Test									
		Paired Differences					t	df	Sig. (2-tailed)
		Mean	Std. Deviation	Std. Error Mean	95% Confidence Interval of the Difference				
					Lower	Upper			
Pair 1	Weight_gr - Ultimate_Tensile_Strength_MPa	–14.663	2.002	.555	–15.872	–13.453	–26.414	12	.000
Pair 2	Weight_gr - Engineering_Strain_mm	5.746	.120	.033	5.673	5.818	172.350	12	.000
Pair 3	Weight_gr - Strain_Force_kN	5.580	.130	.036	5.501	5.658	154.869	12	.000
Pair 4	Weight_gr - Break_Force_Fb_kN	5.076	.166	.046	4.976	5.177	110.020	12	.000
Pair 5	Weight_gr - Break_Stress_Sb_MPa	–13.045	2.337	.648	–14.457	–11.633	–20.129	12	.000
Pair 6	Weight_gr - Elongation_eb_percent	–1.003	1.229	.341	–1.745	–.260	–2.943	12	.012
Pair 7	Weight_gr - Tensile_Modulus_Et_MPa	–633.464	33.400	9.264	–653.648	–613.281	–68.383	12	.000
$p < 0.005$									

After conducting the experimental tests, calculations were performed to optimize the process, simulate different scenarios, and compare the results. The calculation focused on engineering stress and strain. First, the engineering stress-strain curves were generated using equations ISO 527-2:2012 [22].

$$\delta_{\text{eng}} = \frac{F}{\text{A}_0}, \text{ Engineering stress} \quad (1)$$

$$\varepsilon_{eng} = \frac{l - l_0}{l_0}. \text{ Engineering strain} \quad (2)$$

As shown in Tab. 4, the statistical analysis using the "paired sample test" demonstrate that most pairs (except Weight_gr - Elongation_eb_percent) show statistically significant differences between weight and other characteristics of the analysed samples.

3 RESULTS AND DISCUSSION

As can be seen from Tab. 3, there are obvious differences between the infill pattern and the results obtained from the testing of the samples.

The statistical analysis using the "paired sample test" on the paired samples (Tabs. 4 and 5.) show statistically significant differences between weight and other analyzed properties; the same differences are found for infill pattern and other analyzed properties. As can be seen, in Tab. 4, only weight and Elongation do not show statistically significante difference; in Tab. 5, infill pattern and weight and infill pattern and elongation do not show statistically significant differences, suggesting that these three variables are more stable and similar to the Infill Pattern.

3.1 Experimental Engineering Stress-Strain Results

Figs. 4a, 4b, 4c, 4d, and 4e graphically present the experimental results in regard to stress strain engineering for specified samples. In this case, the comparisons focus on samples with varying internal structural designs but can be considered and grouped as samples with approximately similar internal design.

Table 5 Paired sample text according to Infill pattern and Ultimate_Tensile_Strength_MPa; Engineering_Strain_mm; Strain_Force_kN; Break_Stress_Sb_MPa; Elongation_eb_percent; Tensile_Modulus_Et_MPa.

Paired Samples Test									
		Paired Differences					*t*	df	Sig. (2-tailed)
		Mean	Std. Deviation	Std. Error Mean	95% Confidence Interval of the Difference				
					Lower	Upper			
Pair 1	Infill pattern - Ultimate_Tensile_Strength_MPa	–13.468	4.636	1.286	–16.269	–10.666	–10.473	12	.000
Pair 2	Infill pattern - Engineering_Strain_mm	6.941	3.898	1.081	4.585	9.296	6.419	12	.000
Pair 3	Infill pattern - Weight_gr	1.195	3.910	1.084	–1.168	3.558	1.102	12	.292
Pair 4	Infill pattern - Strain_Force_kN	6.775	3.888	1.078	4.426	9.124	6.283	12	.000
Pair 5	Infill pattern - Break_Force_Fb_kN	6.271	3.881	1.076	3.926	8.616	5.827	12	.000
Pair 6	Infill pattern - Break_Stress_Sb_MPa	–11.850	4.296	1.192	–14.446	–9.254	–9.945	12	.000
Pair 7	Infill pattern - Elongation_eb_percent	.192	3.516	.975	–1.932	2.317	0.197	12	.847
Pair 8	Infill pattern - Tensile_Modulus_Et_MPa	–632.269	32.676	9.063	–652.015	–612.523	–69.766	12	.000
$p < 0.005$									

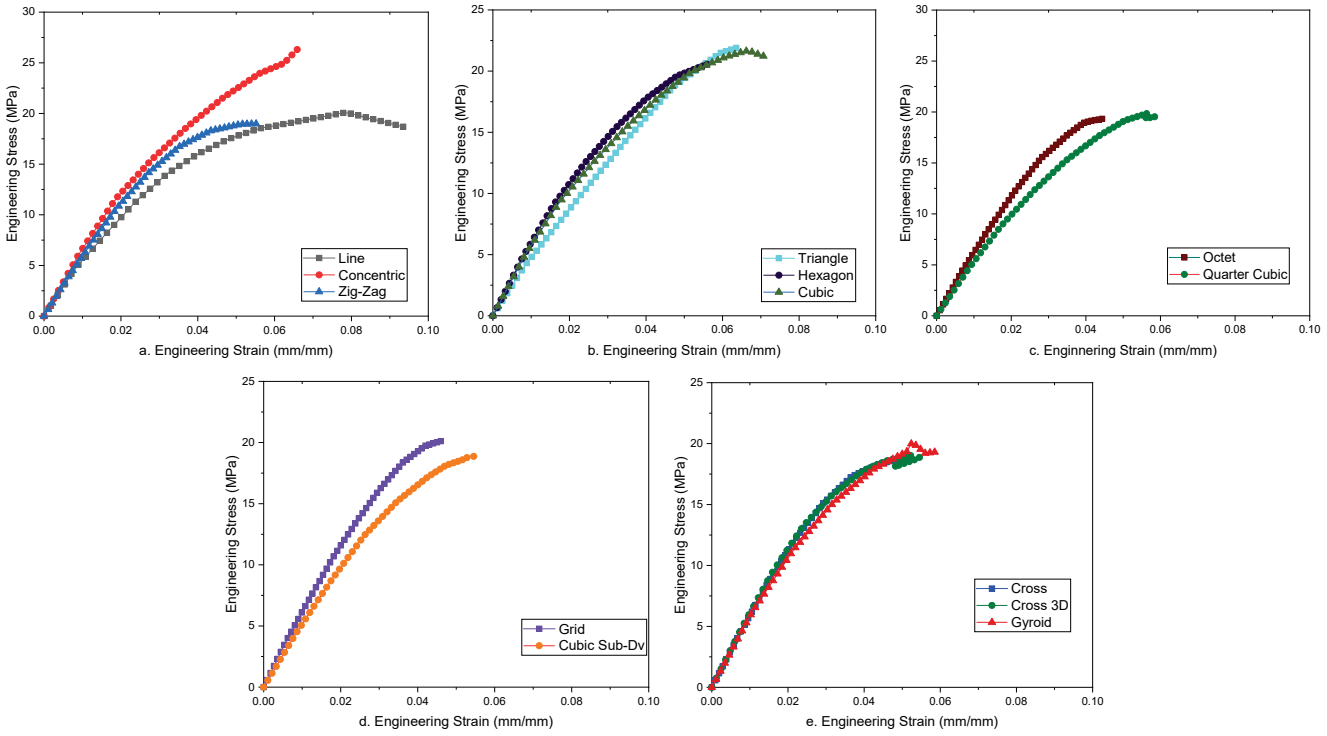

Figure 4 Comparison of samples grouped according to design approximately similar to internal structure mm/mm.

Therefore, their division into groups was made by categorizing them based on their internal shape and comparing them among themselves; comparisons were made for engineering stress strain, where the Fig. 4a shows the comparative results for the samples named Line, Concentric and Zig-Zag, in Fig. 4b the comparative results for Triangle, Hexagon and Cubic samples are presented. Fig. 4c shows the comparative results for the Octet and Quarter Cubic samples, while Fig. 4d shows the comparative results for the Grid and Cubic Subdvision samples, and Fig. 4e shows the comparative results for Cros, Cros 3D and Gyroid samples.

The graphical presentation of the engineering stress-strain curves for the buried samples shows that, with the exception of Fig. 4a, the sample labeled Zig-Zag has a significant difference in terms of stress and strain. In contrast, almost all the lower groups have results that are very close in terms of stress and strain.

3.2 Comparison Results of Ultimate Tensile Strength and Engineering Strain

Comparisons of the results for each sample were made separately for ultimate tensile strength (UTS), expressed in MPa, and for engineering strain, expressed in mm.

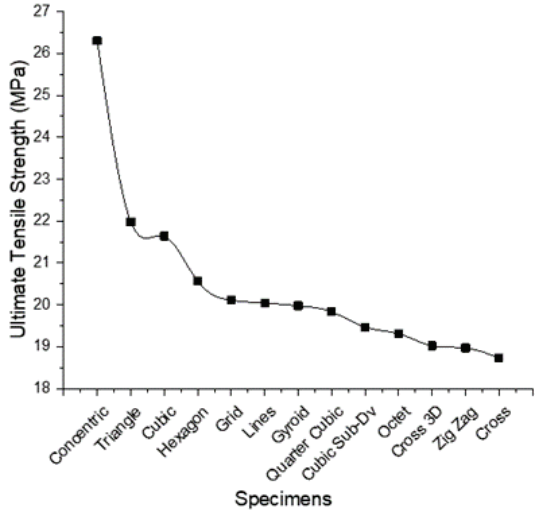

Figure 5 Comparison of samples for Ultimate Tensile Strength (MPa)

Fig. 5 graphically presents the comparative results for Ultimate Tensile Strength (UTS) for the tested samples. It is evident that the highest UTS is presented in the Concentric sample, followed by the Triangle and Cubic samples. In contrast, samples like Hexagon, Gride Line and Gyroid show very similar UTS values. The lowest UTS is found in the Quarter Cubic, Cubic Subdivision, Octet, Cross 3D, Zig-Zag and Cross samples.

Fig. 6 graphically presents the engineering strain results for all samples. In this comparison, the Line infill pattern sample shows a more emphasized elongation than the other samples, while the Concentric, Triangle, and Cubic samples appear to have nearly similar elongation. Whereas samples with approximately similar extension, but lower than those mentioned are Hexagon, Gyroid, Quarter Cubic, Cubic Subdivision, Cross 3D and Zig-Zag. The samples showing the lowest extension are Grid, Octet, and Cross. It is important to note that samples demonstrating a more pronounced elongation do not mean that they have or should have a higher UTS because in this case, the main factor is the internal structural design. Additional statistical comparisons are presented in Tabs. 4 and 5.

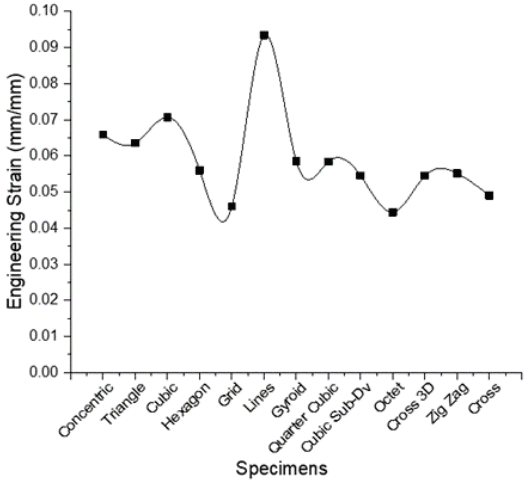

Figure 6 Comparison of samples for Engineering Strain mm/mm

4 CONCLUSIONS

Based on the results of the tested samples, it can be observed that the infill pattern has a particular importance during 3D printing for products that are subject to tensile forces. As seen in Tabs. 4 and 5, most of the samples show statistically significant changes both for the weight of the samples and the infill pattern. The engineering experimental results for stress-strain (Fig. 4) indicate that there are differences among the tested samples as this is evident within the infill pattern groups that are considered roughly similar. Changes were observed in both Engineering Strain (mm) and in Engineering Stress (MPa). Fig. 5 demonstrates that the Concentric filling form shows much higher results in Ultimate Tensile Strength. Meanwhile, Fig. 6 shows that the Line infill pattern displays significantly greater results in engineering strain (mm).

5 REFERENCES

[1] El Mehtedi, M., Buonadonna, P., El Mohtadi, R., Aymerich, F. & Carta, M. (2024). Surface quality related to machining parameters in 3D-printed PETG components. *Procedia Comput. Sci., 232*, 1212-1221. https://doi.org/10.1016/j.procs.2024.01.119

[2] Thakar, C. M., Parkhe, S. S., Jain, A., Phasinam, K., Murugesan, G. & Ventayen, R. J. M. (2022). 3d Printing: Basic principles and applications. *Mater. Today Proc., 51*(1), 842-849. https://doi.org/10.1016/j.matpr.2021.06.272

[3] Vujović, I. (2015). The introduction of 3D printing into the Maritime Industry. *Trans. Marit. Sci., 4*(1), 86-87.

[4] Karad, A. S., Sonawwanay, P. D., Naik, M. & Thakur, D. G. (2023). Experimental study of effect of infill density on tensile

and flexural strength of 3D printed parts. *J. Eng. Appl. Sci., 70*(1), 104. https://doi.org/10.1186/s44147-023-00273-x

[5] Cabreira, V. & Santana, R. M. C. (2020). Effect of infill pattern in Fused Filament Fabrication (FFF) 3D Printing on materials performance. *Matéria (Rio Janeiro), 25*(3). https://doi.org/10.1590/S1517-707620200003.1126

[6] Liacouras, P. C., Huo, E. & Mitsouras, D. (2024). 3D Printing Technologies and Materials. In *3D Printing at Hospitals and Medical Centers: A Practical Guide for Medical Professionals*, Springer, 47-69. https://doi.org/10.1007/978-3-031-42851-7_4

[7] Afonso, J. A., Alves, J. L., Caldas, G., Gouveia, B. P., Santana, L. & Belinha, J. (2021). Influence of 3D printing process parameters on the mechanical properties and mass of PLA parts and predictive models. *Rapid Prototyp. J., 27*(3), 487-495. https://doi.org/10.1108/RPJ-03-2020-0043

[8] Blanco, I. (2020). The use of composite materials in 3D printing. *J. Compos. Sci., 4*(2), 42. https://doi.org/10.3390/jcs4020042

[9] Iftekar, S. F., Aabid, A., Amir, A. & Baig, M. (2023). Advancements and limitations in 3D printing materials and technologies: a critical review. *Polymers (Basel), 15*(11), 2519. https://doi.org/10.3390/polym15112519

[10] Soni, R. D. (2022). Geometric Stability of Parts Produced by 3D Printing. *Tehički vjesnik, 29*(1), 23-29. https://doi.org/10.17559/TV-20191101110214

[11] Dizon, J. R. C., Espera Jr, A. H., Chen, Q. & Advincula, R. C. (2018). Mechanical characterization of 3D-printed polymers. *Addit. Manuf., 20*, 44-67. https://doi.org/10.1016/j.addma.2017.12.002

[12] Kain, S., Ecker, J. V., Haider, A., Musso, M. & Petutschnigg, A. (2020). Effects of the infill pattern on mechanical properties of fused layer modeling (FLM) 3D printed wood/polylactic acid (PLA) composites. *European Journal of Wood and Wood Products, 78*, 65-74. https://doi.org/10.1007/s00107-019-01473-0

[13] Lee, J.-Y., An, J. & Chua, C. K. (2017). Fundamentals and applications of 3D printing for novel materials. *Appl. Mater. Today, 7*, 120-133. https://doi.org/10.1016/j.apmt.2017.02.004

[14] Shahrubudin, N., Lee, T. C. & Ramlan, R. (2019). An overview on 3D printing technology: Technological, materials, and applications. *Procedia Manuf., 35*, 1286-1296. https://doi.org/10.1016/j.promfg.2019.06.089

[15] Anderson, T. L. & Anderson, T. L. (2005). *Fracture mechanics: fundamentals and applications*. CRC press. https://doi.org/10.1201/9781420058215

[16] D. Pezer, F. Vukas, and M. Butir, 2022 "Experimental study of tensile strength for 3D printed specimens of HI-PLA polymer material on in-house tensile test machine. *Technium, 4*(10), 197-206. https://doi.org/10.47577/technium.v4i10.7927

[17] Faidallah, R. F., Hanon, M. M., Vashist, V., Habib, A., Szakál, Z. & Oldal, I. (2023). Effect of Different Standard Geometry Shapes on the Tensile Properties of 3D-Printed Polymer. *Polymers (Basel), 15*(14), 3029. https://doi.org/10.3390/polym15143029

[18] Lalegani Dezaki, M. & Mohd Ariffin, M. K. A. (2020). The effects of combined infill patterns on mechanical properties in FDM process. *Polymers (Basel), 12*(12), 2792. https://doi.org/10.3390/polym12122792

[19] Soufivand, A. A., Abolfathi, N., Hashemi, A. & Lee, S. J. (2020). The effect of 3D printing on the morphological and mechanical properties of polycaprolactone filament and scaffold. *Polym. Adv. Technol., 31*(5), 1038-1046. https://doi.org/10.1002/pat.4838

[20] Đurović, S., Lazarević, D., Milovanović, V., Mišić, M. & Šarkoćević, Ž. (2024). The Influence of the Number of Layers and the Raster Angle on the Mechanical Properties of 3D Printed Materials. *Tehički vjesnik, 31*(6), 1892-1897. https://doi.org/10.17559/TV-20240325001430

[21] Bianchi, I., Mancia, T., Mignanelli, C. & Simoncini, M. (2024). Effect of nozzle wear on mechanical properties of 3D printed carbon fiber-reinforced polymer parts by material extrusion. *Int. J. Adv. Manuf. Technol., 130*(9), 4699-4712. https://doi.org/10.1007/s00170-024-13035-7

Authors' contacts:

Rrahim Sejdiu, Prof. Assoc. Dr.
University of Applied Sciences in Ferizaj - Kosovo,
Str. "University", 70000 Ferizaj, Kosovo
Tel./Fax, e-mail: +38345207276
rrahim.sejdiu@ushaf.net

Xhemajl Mehmeti, Prof. Assist. Dr.
(Corresponding author)
University of Business and Technology,
Lagjja Kalabria, 10000 Prishtine - Kosovo
Tel./Fax, e-mail: +38344981727
xhemajl.mehmeti@ubt-uni.net

Flamur Salihu, Prof. Assist. Dr.
University of Applied Sciences in Ferizaj - Kosovo
Str. "University", 70000 Ferizaj, Kosovo
Tel./Fax, e-mail: +38344428613
flamur.salihu@ushaf.net

Labinot Topilla, Prof. Assist. Dr.
University of Applied Sciences in Ferizaj - Kosovo,
Str. "University", 70000 Ferizaj, Kosovo
Tel./Fax, e-mail: +38344698611
labinot.topilla@ushaf.net

Drin Krasniqi, MSc.
University of Pristina,
"George Bush", Nr. 31, 10000 Prishtine - Kosovo,
Tel./Fax, e-mail: +38348800882
drin.krasniqi@uni-pr.edu

Mohamad El Mehtedi, Prof. Dr.
University of Cagliari,
Via Marengo, 2, 09123 Cagliari - Italia
Tel./Fax, e-mail: +39 070 675 5721
m.elmehtedi@unica.it

Agron Bajraktari, Prof. Dr.
University of Applied Sciences in Ferizaj - Kosovo,
Str. "University", 70000 Ferizaj, Kosovo
Tel./Fax, e-mail: +38345999666
agron.bajraktari@ushaf.net